JOURNAL OF SPACECRAFT AND ROCKETS
Vol. 31, No. 6, November–December 1994

Direct Simulation Monte Carlo Simulation of the Interaction Between Rarefied Free Jets

Leonardo Dagum*
NASA Ames Research Center, Moffett Field, California 94035
and
S. Konrad Zhu†
Rockwell International Corporation, Canoga Park, California 91303

This paper presents a direct simulation Monte Carlo (DSMC) calculation of two interacting free jets exhausting into vacuum. The computed flow field is compared against available experimental data and shows excellent agreement everywhere except in the very near field (less than one orifice diameter downstream of the jet exhaust plane). The lack of agreement in this region is attributed to having assumed an inviscid boundary condition for the orifice lip. The results serve both to validate the DSMC code for a very complex, three-dimensional, nonequilibrium flowfield, and to provide some insight into the complicated nature of this flow.

Introduction

THE study of interactions of adjacent parallel jets underexpanded into a vacuum chamber has been an interesting research subject area of rarefied gas dynamics in the past. Its engineering applications are mostly related to the design of spacecraft. The recent resurgence of interest in the subject is prompted by the design of Space Station Freedom. The possible excessive loads on the solar panel of the station due to the Orbiter reaction control system (RCS) plume impingement are of a great concern. In particular, the determination of the plume flowfield resultant from multiple RCS engine firings has been difficult and highly uncertain. Thus, the analysis of the impingement problem related to multiple RCS plumes is a major source of uncertainty in the space-station design.

In a previous paper,[1] the results from a direct simulation Monte Carlo (DSMC) analysis have indicated that there is still a significant interaction between two RCS plumes separated even by a distance of 60 ft. The implication is highly relevant to the space-station design. It suggests that predicting the multiple-plume flowfield as a linear superposition of the single plumes from the RCS engines is highly inaccurate even for the largest nozzle separation distance on the Orbiter. Clearly, there is a need for better understanding of the plume interaction problem before designs based on superposition can be accepted with confidence.

Naturally, validation of the computer code used in the simulations of Ref. 1 with proper experimental data is desirable. Considering the thrust level of the RCS engine (870 lbf) and its operation conditions (340-km altitude), a parametric study in ground chamber testings would be extremely difficult if not impossible. A flight test in space is seemingly attractive, and such a test has been proposed by the space-station design team. However, because of the budgetary and scheduling problems, the proposed test has yet to be carried out. Even upon commencement of the proposed flight test, the data collected by the Remote Manipulate System (the robot arm), which is restricted in its range and loading limit, will be of value only for validation of the single-RCS-plume flowfield calculation in the far field. Thus the only alternative available for validation of plume interaction calculations is to simulate well-documented experimental works focused on the interactions between two rarefied free jets, such as in Refs. 2 and 3. To date there have been few studies comparing DSMC nozzle flow solutions with experiment (see Refs. 4–7). Furthermore, these few studies have focused exclusively on single-nozzle flows. The current work examines multiple-plume flowfields in a general three-dimensional framework and makes direct comparison with experimental measurements.

In choosing the data to be used for the code validation, it is realized that data from an intrusive probing measurement, such as the Patterson probe employed in Ref. 2, needs a separate simulation on the characteristics of the probe as a function of the rarefactions of testing jets as a prerequisite for using the measured data as the base of the code validation. The data from a nonintrusive measurement better serves the purpose of the validation. The work performed by Soga et al.[3] employed the electron-beam technique to measure the interactions of two parallel nitrogen jets from sonic orifices into vacuum. The intensity of the emissions varies with the density of the flowing gas. Thus, the recording of the emission intensity reflects the structure of the flowfield. The present work is to simulate the experiment carried out by Soga et al. and to compare the simulation results with the data reported in Ref. 3.

Computational Method

The data-parallel algorithms used for the present work are described in Refs. 1 and 8. The computer code itself is largely unchanged from the one employed in Ref. 1. Some capabilities have been added to more closely simulate the conditions used in the experiments. In particular, the code can simulate the jet flow in a finite background pressure as well as in a vacuum, and the flow simulation can either start immediately at the sonic orifice exit plane or be initiated from a starting surface away from a nozzle exit plane (as in Ref. 1). Most importantly, the code now also has the capability of automatically adapting the grid cells to better resolve the flow and to extend the downstream distance that can be simulated.

In Ref. 1, a solution by the method of characteristics (MOC) was invoked to generate the starting surface for the sake of calculation efficiency. The same strategy is not employed here, because the jets in the experiments were very closely placed and there is little to be gained by using an MOC solution for a starting surface. In the present work, the simulation is started at the the sonic orifice with particles introduced at a constant rate and at sonic conditions. It is well known that for highly underexpanded free jets, the high supersonic region is only weakly dependent on the transonic exit conditions[9–11]; therefore it is safe to assume that a small discrepancy between orifice exit conditions in the simulation and in the experiments does not lead to larger discrepancies downstream.

The major change made to the code is the capability to adapt itself to the flow. This is accomplished through the use of cell "groupings" similar to the approach described in Ref. 12. Following Rault et al.[12] the computational grid has two levels: a uniform background

Received Aug. 17, 1993; revision received Feb. 17, 1994; accepted for publication Feb. 21, 1994.

*Currently with Computer Sciences Corp. Member AIAA.
†Rocketdyne Division. Member AIAA.

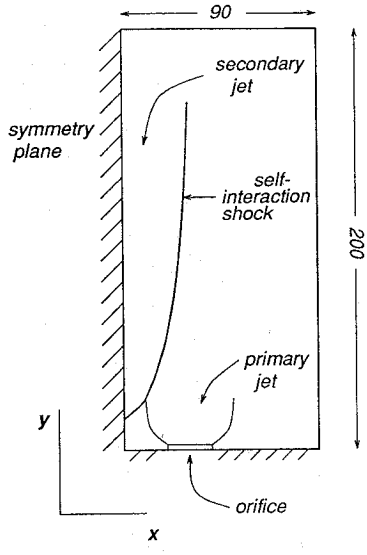

Fig. 1 Geometry for DSMC simulation.

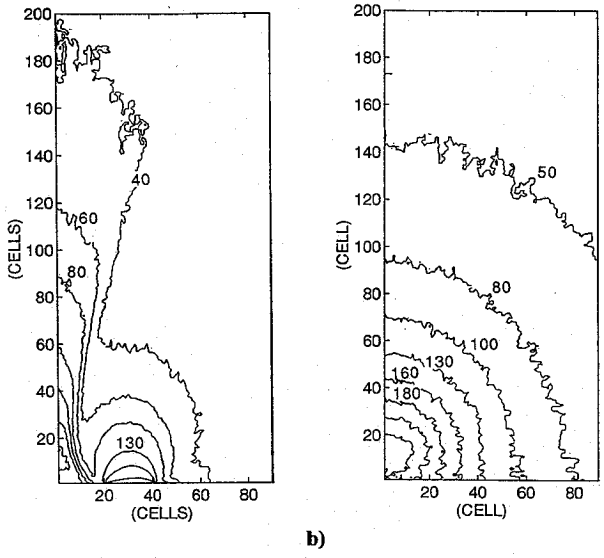

Fig. 2 Density contours (labels in units of 2.33 × 10^{-5} kg/m^3): a) *x-y* plane and b) *y-z* (symmetry) plane.

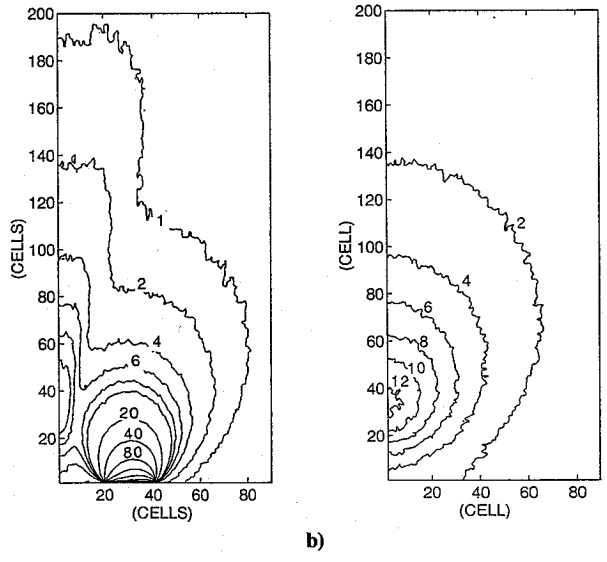

Fig. 3 Translational temperature contours (labels in Kelvins): a) *x-y* plane and b) *y-z* (symmetry) plane.

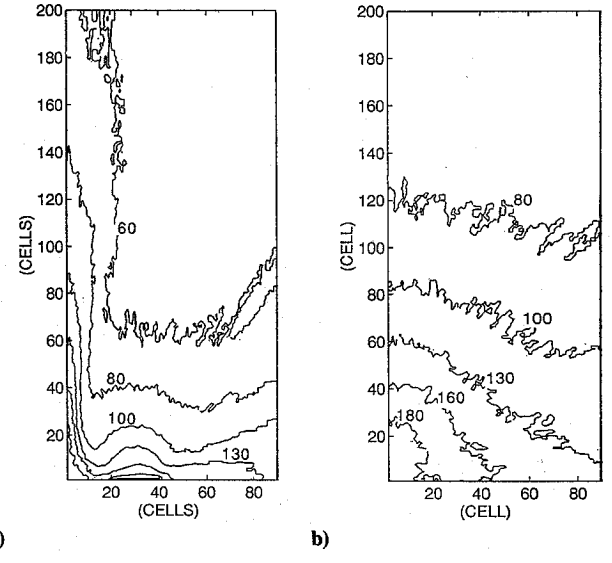

Fig. 4 Rotational-temperature contours (labels in Kelvins): a) *x-y* plane and b) *y-z* (symmetry) plane.

Cartesian mesh and a superimposed computational grid made from grouping the background mesh cells. To start the simulation, a mapping of background cells to groups is either read in externally or generated automatically. In the latter case, the mapping results in a straight grouping of background cells into blocks of size $i \times j \times k$, where i, j, k are input values. In a typical case, the code is run through the transient with these blocks for computational cells. An approximate solution is generated, and this is used then to adapt the grid.

In the current work, just the density is used for adaptation, although any scalar quantity may be employed. The algorithm used is simply a weighted recursive coordinate bisection. The procedure is to bisect the background mesh to create two submeshes of approximately equal weight (based on the density in this case). Each submesh is then bisected in the same manner, and this is repeated until the desired number of "submeshes" (i.e., groups) are created. The procedure is a little restrictive in that one can only ask for a power-of-two number of cell groups, and often one obtains a number somewhat less than this because the code will not bisect a submesh consisting of a single background cell. The technique is attractive, however, because it is very fast and it produces parallelepiped cell groups. The major advantage of parallelepiped cell groups is that it allows for the efficient implementation of a variable time step. For particles that cross into regions of differing time steps it is necessary to compute the distance traveled in the two regions in order to correct the particle position. This calculation can be very efficient with the parallelepiped cell groups. Variable time steps were not employed in the current calculations, although the capability has been added to the code. There is some question of the accuracy with particles moving between regions of very different time step (e.g; from $\Delta t = 1.0$ to $\Delta t = 2.0$), and a suitable smoothing of the time steps has yet to be included. The code does allow for a global change in time step, which is useful in going from an initial block grouping to an adapted grid.

Problem Description

Figure 1 shows the geometry for the simulation. The parameters were set to simulate the experimental results[3] for a separation distance of 3.0 orifice diameters (i.e., 9 mm) with molecular nitrogen as a test gas. The stagnation temperature and pressure were set to 285 K and 870 Pa, respectively. The experiment had a back pressure of 3.7 Pa, but the simulation used a vacuum because the large computational domain required too many particles to maintain a back pressure. Near-field simulations carried out with a back pressure confirmed that the back-pressure gas made a negligible contribu-

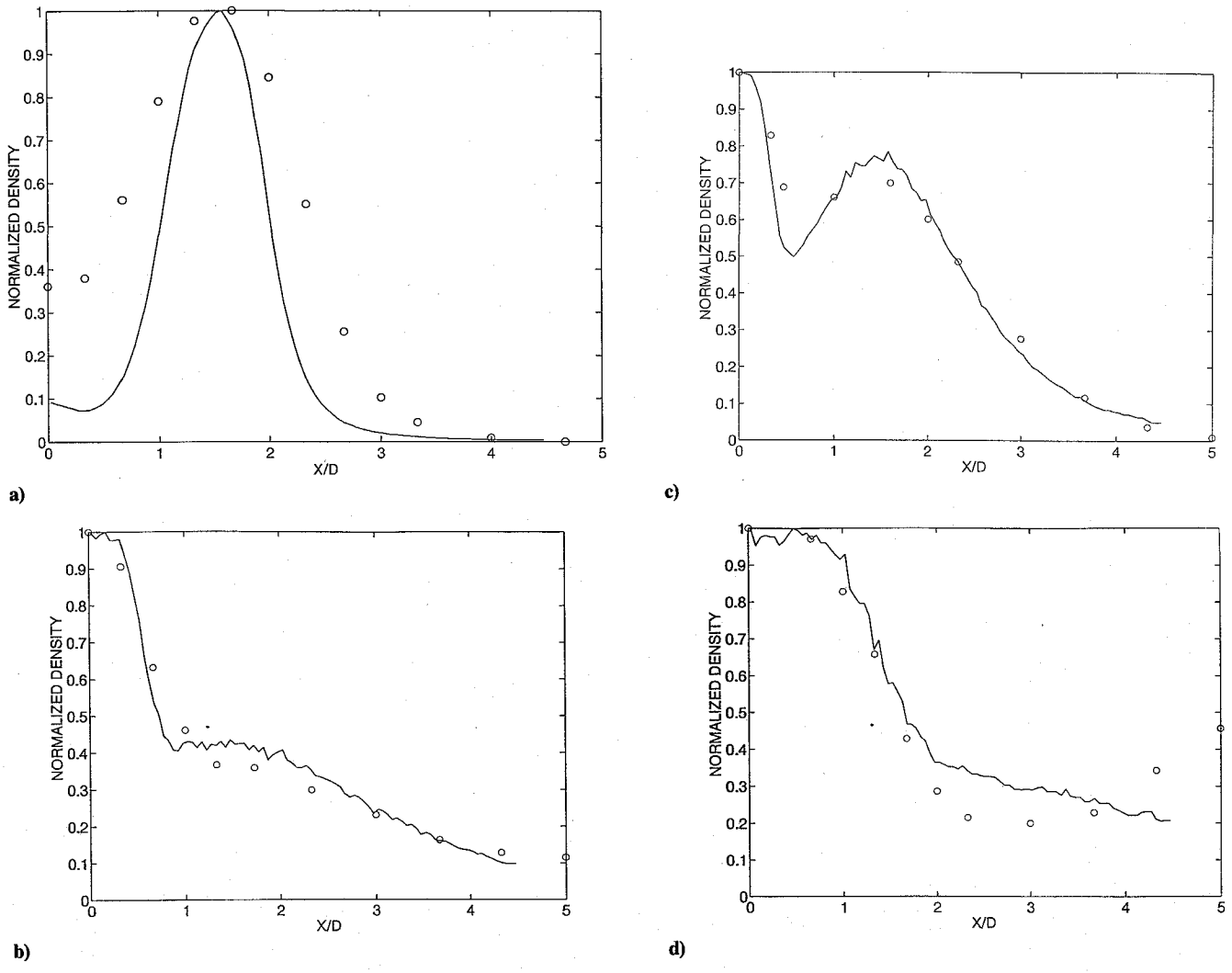

Fig. 5 Density profile along x axis at: y/D = a) 0.6, b) 2.0, c) 3.3, and d) 6.4.

tion to the near-field flow. The back-pressure gas does affect the far-field results, especially about the Mach disk and beyond, but the simulation domain did not extend so far. The hard-sphere Knudsen number at the orifice exit, based on the orifice diameter, is 0.00385. The simulation assumed an inverse ninth-power law for nitrogen. Internal energy is relaxed through the Borgnakke-Larsen model, using a fixed rotational collision number of 5.

The simulated orifice had a diameter of 20 cells, and its center was placed 30 cells from the interaction plane. The orifice exit plane was 1 cell above the specular reflecting boundary at $y = 0$ (see Fig. 1). Raising the orifice exit plane at least 1 cell is required by the code. In the experiment the two orifices were flush with a back plate. The background grid had dimensions $90 \times 200 \times 90$. The simulation was started with $2 \times 2 \times 2$ block groups for a total of 202,500 groups.

The hard-sphere mean free path at the orifice exit plane was 0.077 cells. It is usually assumed that DSMC solutions are accurate only where the mean free path is at least as great a cell dimension. However, grid-resolution studies performed by Haas[13] for compressing flows have shown that, in the case of a boundary layer, coarse grids do not restrict flow gradients and coarse-grid solutions track the fine-grid solution quite accurately. For an expanding flow it is reasonable to expect the DSMC solution will expand at the correct rate and so become "accurate" at points downstream where the mean free path is greater than the cell dimension. For this calculation, the mean free path is equal to the cell size on an ellipsoidal surface centered at the orifice (i.e., with semiminor axis equal to half the orifice diameter) and extending to 0.80 diameters downstream. It is safe to conclude that the calculation is accurate outside this region.

The simulation was run for 2000 steps before adapting. This was enough to allow a fluid particle to travel two lengths of the computational domain and thereby for the simulation to reach steady state. Furthermore, between 1800 and 2000 steps the number of particles in the flow changed by 0.01%, a good indication that steady state had been reached. In between, particles were cloned twice, first after 800 steps and then again at 1200 steps. After adaptation there were 373,355 cell groups and 2.22 million particles (adaptation doubled the number of particles, as the time step was halved in going from the block groups to the adapted groups). The simulation was run a further 100 steps to clear out any residual effects from adapting the grid, and then time-averaged for a total of 2600 steps with samples collected every time step.

The calculation was performed on 64 nodes of the Thinking Machines Connection Machine CM-5 at the Numerical Aerodynamic Simulation (NAS) facility in NASA Ames Research Center. The entire calculation required 13.4 CPU hours to complete, with the transient accounting for 1.8 h. The average particle update time with block groups and time averaging was 3.8 μs, and with adapted groups and time averaging was 6.5 μs. The adapted groups require a level of indirection to determine in which cell group a particle belongs. This adds a substantial amount of interprocessor communication, and at the time of the calculation no effort had yet been made to optimize this part of the code.

Results

Figures 2–4 present the density and translational- and rotational-temperature fields for two planes of the simulation: 1) the x-y plane, or the plane through the orifice axis and 2) the y-z plane, or the symmetry plane. The existence of a secondary jet at the centerline is clearly visible in the x-y-plane results. The secondary jet is created from the interaction of the two primary jets (associated with the real

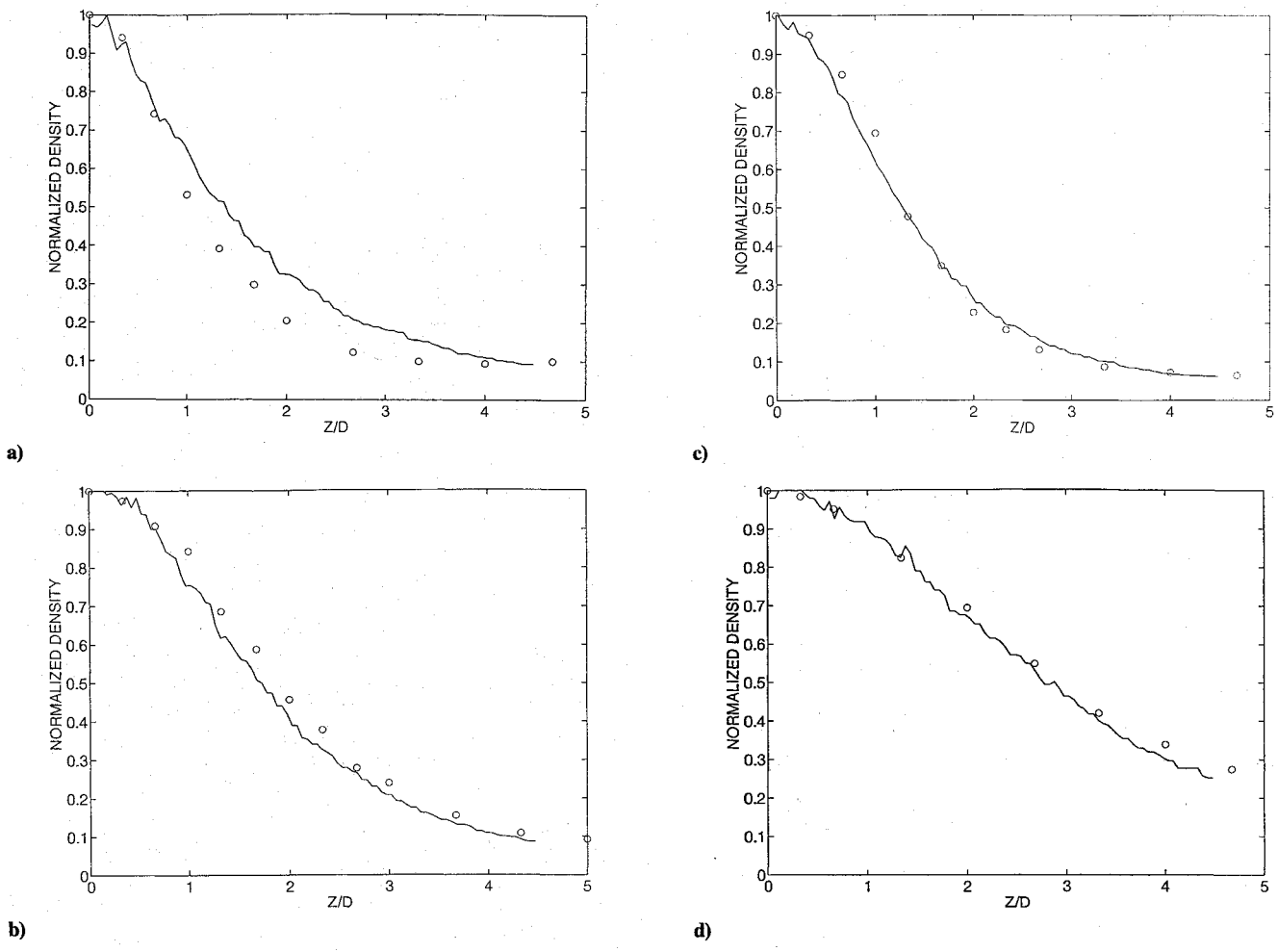

Fig. 6 Density profile along z axis at: y/D = a) 0.5, b) 1.2, c) 2.4, and d) 4.5.

and virtual orifices in the simulation) at the symmetry plane. The jet begins about half a diameter downstream of the orifice plane. Looking at Fig. 2a, one can see the jet interaction shock clearly marking the secondary jet boundary; the primary jet has no such shock associated with it. Note the jet interaction shock crosses over the center of the primary jet approximately 5 diameters downstream of the orifice plane. The translational temperature noticeably leads the density shock, crossing over the primary jet at roughly 4 diameters downstream. The rotational temperature (see Fig. 4a) follows the density more closely in the secondary jet. The primary-jet expansion and mixing at the interaction plane both contribute to create a region of very high thermal nonequilibrium, as is seen in the figures.

Looking at the corresponding results in the y-z (symmetry) plane, the three-dimensional nature of the flow is clearly evident. The secondary jet does not exhibit the radial symmetry associated with a free jet. In Fig. 2b it is clear that the secondary jet is quite broad in the direction transverse to the primary jets, whereas it is rather constrained between the two jets. Note that the peak density in the secondary jet occurs about 1.8 diameters (see Fig. 7a) downstream of the orifice plane. In contrast, the peak translational temperature occurs only 0.8 diameters downstream, and the peak rotational temperature occurs at the orifice plane. It would appear as though rotational temperature were leading translational temperature; however, looking at Fig. 4a, one can see that unlike the translational-temperature, the rotational temperature in the primary jet actually increases at the higher off-center angles (because of rotational energy freezing through the expansion). For this reason the secondary jet has its peak rotational temperature at the orifice plane (see also Fig. 7b).

Figures 5a–5d present density profiles along the x axis at 0.6, 2.0, 3.3, and 6.4 diameters downstream of the orifice. For purposes of comparison, both the experimental and the numerical results have been normalized by their peak values. The experiment density measurements were made through electron-beam fluorescence, which measures only changes in density and so does not yield quantitative data. Therefore normalizing by the peak values is appropriate. Symbols are used to represent experimental results. Additional results may be found in Ref. 14.

Except for the very near field (i.e., less than 1 diameter from the orifice plane) the agreement between the simulation and the experiment is remarkable. In the very near field, the simulation predicts a much lower density at the centerline than was measured in the experiment. Furthermore, the density peak going over the orifice is sharper than measured. This is evident in Fig. 5a at 0.6 diameters downstream, and to a lesser degree at 1.3 diameters (see Ref. 14). The lack of agreement in the very near field is attributed to a boundary-layer effect at the orifice lip. Since the calculation assumed an inviscid orifice and back plate (i.e., specular reflection), it failed to allow for the boundary layer that would develop at the orifice lip in a real flow. It is expected that a boundary layer at the orifice lip would increase the flow at the large off-axis angles (see Ref. 15) and so contribute to a greater density there. This would have the effect of raising the density at the centerline of two interacting free jets, and correspondingly reducing the peak density over a single jet. Because of the normalization used in presenting these results, the latter effect would result in the "wider" peak seen at 0.6 diameters (Fig. 5a).

The simulation results also diverge from experiment in Fig. 5d at positions greater than 4 diameters from the interaction plane. At this downstream location the secondary jet dominates the flow and no evidence of the primary jet remains. Moving away from the interaction plane, the experiment shows a rise in density corresponding to the very thick barrel shock that exists at this downstream location. The simulation did not generate a barrel shock, because no back pressure was introduced, and so the simulation results diverge from the experiment here.

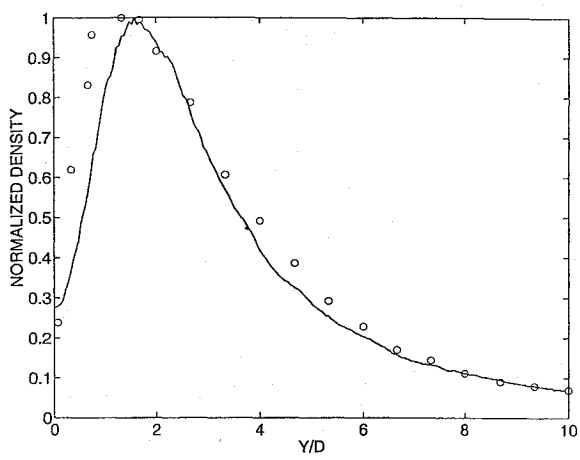

a)

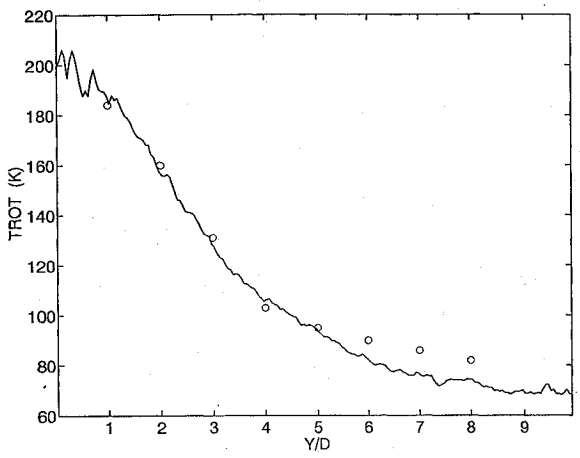

b)

Fig. 7 a) Density distribution and b) rotational temperature distribution along centerline (0, y, 0).

Figures 6a–6d present density profiles along the z axis at 0.5, 1.2, 2.4, and 4.5 diameters downstream of the orifice. Again the results have been normalized by the peak values. As with the results along the x axis, the agreement is excellent except at the very near field. Additional results may be found in Ref. 14. For the very near field (Fig. 6a) the experimental results show a higher density than the calculation, which, because of the normalization, appears as a "narrower" peak in the figures. This may be explained by the orifice lip boundary layer as discussed above.

Figures 7a and 7b present the density and rotational temperature distributions along the centerline [the (0, y, 0) line]. There is generally good agreement. Both the experiment and the simulation show the peak density occurring at 1.8 diameters downstream, corresponding to 40 deg from the orifice axis. The simulation, however, exhibits a slightly sharper density rise and drop, which indicates that it is overpredicting the peak density value. This would be consistent with the earlier observations on the effect of the orifice lip boundary layer. By increasing the flow at the higher angles the boundary layer reduces flow at the medium angles that contribute to the peak density in the interaction plane.

Experimental measurements for rotational temperature were started only after one diameter from the orifice plane, and so boundary-layer effects are not apparent. As discussed above, the peak rotational temperature along the centerline occurs at the orifice plane. The mechanism producing this result (i.e., rotational-energy freezing in the gas expansion) would not be so pronounced in the presence of a boundary layer at the orifice lip, so for the viscous orifice the peak rotational temperature along the centerline may occur further downstream.

Overall the simulation shows remarkably good agreement with experimental results. As expected, differences between the experimental and simulated orifice exit conditions do not have a significant affect on the high supersonic region further downstream. These results provide some measure of confidence in applying the technique to conduct a parametric study of multiple RCS engine firings of the Orbiter and should allow the development of more accurate engineering models for this complex flow.

Conclusions

The interaction of two free jets results in the creation of a secondary jet centered between the two primary jets. A complicated, three-dimensional, highly nonequilibrium flowfield ensues. This flowfield has been accurately simulated with a DSMC calculation. The computed flowfield is compared against available experimental data and shows excellent agreement everywhere except in the very near field (less than one orifice diameter downstream of the jet exhaust plane). The lack of agreement in this region is attributed to differing orifice exit conditions. Specifically, the simulation assumes an inviscid boundary condition for the orifice lip, whereas in the real flow a boundary layer will develop. The results serve both to validate the DSMC code and to provide some insight into the complicated nature of this flow. The method may now be used with some confidence to conduct a parametric study of multiple RCS engine firings on the Orbiter.

Acknowledgments

The work of Leonardo Dagum was sponsored under NASA contract NAS-2-12961, and that of S.Konrad Zhu under NASA contract NASA 8-251082. The authors thank Professors M. Yasuhara and T. Soga of Nagoya University for kindly providing the experimental data for the free-jet interaction.

References

[1]Dagum, L., and Zhu, S. K., "Three Dimensional Particle Simulation of High Altitude Rocket Plumes," AIAA Paper 92-2913, July 1992.

[2]Dankert, C., and Koppenwallner, G., "Experimental Study of the Interaction between Two Rarefied Free Jets," *14th International Symposium on Rarefied Gas Dynamics*, Vol. 1, edited by H. Oguchi, Tsukuba Science City, Japan, 1984, pp. 477–484.

[3]Soga, T., Takanishi, M., and Yasuhara, M., "Experimental Study of Underexpanded Free Jets," *14th International Symposium on Rarefied Gas Dynamics*, Vol. 1, edited by H. Oguchi, Tsukuba Science City, Japan, 1984, pp. 485–493.

[4]Boyd, I. D., Penko, P. F., and Meissner, D. L., "Numerical and Experimental Investigations of Rarefied Nozzle and Plume Flows of Nitrogen," AIAA Paper 91-1363, June 1991.

[5]Penko, P. F., Boyd, I. D., Meissner, D. L., and DeWitt, K. J., "Measurement and Analysis of a Small Nozzle Plume in Vacuum," AIAA Paper 92-3108, July 1992.

[6]Campbell, D. H., "DSMC Analysis of Plume-Freestream Interactions and Comparison of Plume Flowfield Predictions with Experimental Measurements," AIAA Paper 91-1362, June 1991.

[7]Campbell, D. H., "High Altitude Plume-Freestream Interaction Flowfields: Comparison of DSMC Predictions with Experimental Measurements," AIAA Paper 92-2857, July 1992.

[8]Dagum, L., "On the Suitability of the Connection Machine for Direct Particle Simulation," Ph.D. Thesis, Dept. of Aeronautics and Astronautics, Stanford Univ., Stanford, CA, June 1990.

[9]Ashkenas, H., and Sherman, F., "The Structure and Utilization of Supersonic Free Jets in Low Density Wind Tunnels," *Proceedings of the 4th International Symposium on Rarefied Gas Dynamics*, Vol. 2, edited by J. H. de Leeuw, Toronto, 1964, pp. 84–105.

[10]Sherman, F. S., Lockheed Missiles and Space Co., Report 6-90-63-61, June 1963.

[11]Anderson, J., Foch, J., Shaw, M., Stern, R., and Wu, B., "Monte Carlo Simulation of Free Jet Flow from a Slit," *15th International Symposium on Rarefied Gas Dynamics*, Vol. 1, edited by V. Boffi and C. Cercignani, Grado, Italy, 1986, pp. 442–451.

[12]Rault, D. F. G., Wilmoth, R. G., and Bird, G. A., "An Efficient DSMC Algorithm Applied to a Delta Wing," AIAA Paper 91-1316, June 1991.

[13]Haas, B., "Flow Resolution and Domain Influence in Rarefied Hypersonic Blunt-Body Flows," AIAA Paper 93-2806, July 1993.

[14]Dagum, L., and Zhu, S. H., "DSMC Simulation of the Interaction between Rarefied Free Jets," AIAA Paper 93-2872, July 1993.

[15]Bird, G. A., "Breakdown of Continuum Flow in Freejets and Rocket Plumes," *12th International Symposium on Rarefied Gas Dynamics*, Vol. 2, edited by S. S. Fisher, Charlottesville, VA, 1980, pp. 681–694.